information

Article

Engineering Four-Qubit Fuel States for Protecting Quantum Thermalization Machine from Decoherence

Fatih Ozaydin [1,*], Ramita Sarkar [2], Veysel Bayrakci [3], Cihan Bayındır [4,5], Azmi Ali Altintas [6] and Özgür E. Müstecaplıoğlu [7,8,9]

1 Institute for International Strategy, Tokyo International University, Higashi-Ikebukuro 4-42-31, Toshima-ku, Tokyo 170-0013, Japan
2 Indian Institute of Science Education and Research Kolkata, Mohanpur 741246, India; ramita.sarkar@iopb.res.in
3 Faculty of Engineering and Natural Sciences, Isik University, Sile, İstanbul 34980, Türkiye; 218ee2189@isik.edu.tr
4 Engineering Faculty, İstanbul Technical University, Sarıyer, İstanbul 34469, Türkiye; cbayindir@itu.edu.tr
5 Engineering Faculty, Boğaziçi University, Bebek, İstanbul 34342, Türkiye
6 Department of Physics, Faculty of Science, İstanbul University, Vezneciler, İstanbul 34116, Türkiye; azmi.altintas@istanbul.edu.tr
7 Department of Physics, Koç University, Sarıyer, İstanbul 34450, Türkiye; omustecap@ku.edu.tr
8 TÜBİTAK Research Institute for Fundamental Sciences, Gebze 41470, Türkiye
9 Faculty of Engineering and Natural Sciences, Sabanci University, Tuzla, İstanbul 34956, Türkiye
* Correspondence: fatih@tiu.ac.jp

Abstract: Decoherence is a major issue in quantum information processing, degrading the performance of tasks or even precluding them. Quantum error-correcting codes, creating decoherence-free subspaces, and the quantum Zeno effect are among the major means for protecting quantum systems from decoherence. Increasing the number of qubits of a quantum system to be utilized in a quantum information task as a resource expands the quantum state space. This creates the opportunity to engineer the quantum state of the system in a way that improves the performance of the task and even to protect the system against decoherence. Here, we consider a quantum thermalization machine and four-qubit atomic states as its resource. Taking into account the realistic conditions such as cavity loss and atomic decoherence due to ambient temperature, we design a quantum state for the atomic resource as a classical mixture of Dicke and *W* states. We show that using the mixture probability as the control parameter, the negative effects of the inevitable decoherence on the machine performance almost vanish. Our work paves the way for optimizing resource systems consisting of a higher number of atoms.

Keywords: entanglement; coherence; Dicke states; *W* states; quantum thermodynamics; quantum heat engines; quantum thermalization machine, master, cavity-QED

check for updates

Citation: Ozaydin, F.; Sarkar, R.; Bayrakci, V.; Bayındır, C.; Altintas, A.A.; Müstecaplıoğlu, Ö.E. Engineering Four-Qubit Fuel States for Protecting Quantum Thermalization Machine from Decoherence. *Information* **2024**, *15*, 35. https://doi.org/10.3390/info15010035

Academic Editors: Wenbin Yu, Yadang Chen and Chengjun Zhang

Received: 27 November 2023
Revised: 29 December 2023
Accepted: 8 January 2024
Published: 10 January 2024

Copyright: © 2024 by the authors. Licensee MDPI, Basel, Switzerland. This article is an open access article distributed under the terms and conditions of the Creative Commons Attribution (CC BY) license (https://creativecommons.org/licenses/by/4.0/).

1. Introduction

Exploring the potentials of quantum resources such as entanglement [1], discord [2] and coherence [3] in enabling quantum tasks is at the heart of quantum information science. Quantum entanglement is required for many tasks such as quantum teleportation and quantum key distribution [4], and quantum discord can be utilized as a resource for quantum communications [5] and remote state preparation [6]. Coherence has been identified as a key resource in the emerging field of quantum thermodynamics, making a breakthrough in the interplay between quantum information and thermodynamics of quantum systems [7,8]. Based on the reversibility of quantum dynamics which turns out to be a central issue in quantum thermodynamics [9], Bender et al. presented a quantum Carnot engine [10], and Abe showed how to maximize its power [11]. In their pioneering work, Scully et al. showed the possibility of constructing a quantum Carnot engine using

the quantum coherence of a three-level atom as the resource in ideal conditions [12], which led to a vast amount of works on quantum information and thermodynamics. Describing the isochoric and isothermal processes in the quantum domain, Quan et al. defined quantum versions of Carnot and Otto engines [13]. Quantum version of the Stirling cycle was also defined [14], and its performance was compared against quantum Otto cycle [15]. Mukherjee et al. showed that the anti-Zeno effect can provide advantages in quantum heat engines [16], and based on atomic collisions, Bouton et al. realized a quantum heat engine [17].

Bound entanglement [18,19], which is irreversible by definition [20], as well as q-deformation associated with the nonlinearity of the system are also a cradle of research in the interplay of quantum information and quantum thermodynamics. Horodecki et al. asked whether utilizing bound entangled states can make entanglement theory reversible and satisfy the laws equivalent to thermodynamics, and they showed it is not possible in general [21]. Tuncer et al. showed the possibility of extracting heat and work from bound entangled states. Lavagno studied quantum thermodynamics with q-deformed bosons and fermions [22], and he showed that they exhibit quantum statistical effects stronger than their non-deformed counterparts [23]. It was recently shown that a quantum Otto engine can be powered only by the deformation of the working substance [24]. While it was questioned whether the Carnot limit can be surpassed by utilizing quantum resources [25–27], Gardas and Deffner showed that it is not allowed by the laws of thermodynamics [28].

The drawback of the engine proposed in Ref. [12] was that it suffers from devastating decoherence. Hence, considering the realistic conditions, in order to beat the decoherence, the state space of the resource should be expanded such as by considering multi-particle entangled systems [29,30], where quantum information becomes even more crucial for quantum thermodynamics.

In the case of a two-qubit quantum system, four orthogonal Bell states can be observed which are equivalent in the sense that they can be transformed to each other by local operations and classical communications [4]. However, two inequivalent states, i.e., GHZ and W states, can be observed in a three-qubit system [31]. In addition to the GHZ and W states, a quantum system of four or more qubits can be in a state in a richer set, such as Dicke states as the generalization of W states [32], or cluster (graph) states [33]. Quantum information theoretic properties and the usefulness of of multiparticle entangled states realizing quantum tasks have received particular attention. In the magic square game, a specific four-qubit state is required to surpass the classical success probability [34]. Graph states are required for the measurement-based quantum computation [35] and communications [36], and it was shown that quantum logic operations can be realized with significantly fewer qubits if weighted graph states are used [37]. GHZ states are required for reaching consensus in quantum networks, while W states are required for electing leaders in anonymous quantum networks [38]. In quantum metrology, GHZ states outperform W states [39]. Therefore, efficient methods for the preparation of these states appear as a key step in quantum science and technologies. While the preparation of GHZ and graph states of an arbitrary number of qubits is straightforward [4], various approaches were designed for the preparation of large-scale W states such as the fusion of smaller W states or expanding a W state with initially separable qubits (see Ref. [40] and references therein).

Nevertheless, designing the state of a quantum resource for realizing a particular quantum task and designing the setup to prepare that state are necessary but not sufficient when the realistic conditions are considered. The decoherence of quantum systems due to inevitable interactions with the environment is devastating for any task, including the building of practical quantum computers. In particular, the ambient temperature is the biggest problem in various technologies, requiring working in ultracold conditions [41,42].

This fact highlights the importance of research on open quantum systems in general. See Refs. [43,44] for a comprehensive review on recent theoretical and experimental works on open quantum systems. In quantum thermodynamics, Zhang et al. have recently studied the impact of one-way multipartite correlations [45]. Taking into account the

friction in the system, Cakmak et al. recently showed how to produce more useful work in quantum Otto and Carnot cycles by coupling an arbitrary spin-s with spin-1/2 for the working substance [46]. To overcome the decoherence, Turkpence and Müstecaplıoğlu generalized the phaseonium by considering a multi-level system [47], and Gassab et al. proposed a geometrical optimization of spin clusters [48]. Recently, superradiance has also been studied in quantum heat engines both theoretically [49] and experimentally [50]. Very recently, the relativistic version of a quantum Otto engine has been studied for extracting instant work [51].

Designing error-correcting quantum codes [52,53] and decoherence-free subspaces [54,55] as well as performing frequent measurements for exploiting the quantum Zeno effect [56,57] are the basic strategies for minimizing the effect of the decoherence on the quantum task's performance. Yamamoto et al. showed that adding an extra qubit to the system can protect it against collective noise in a simpler and more flexible way than the decoherence-free subspace approach [58]. Along this vein, machine learning techniques have also been developed recently [59,60]. In this work, we propose an alternative strategy. By carefully analyzing the effect of the decoherence on the resource system, we design its quantum state, introducing a control parameter that can be tuned accordingly to protect the task's performance from the effect of decoherence.

Dag et al. considered a quantum thermalization machine consisting of an optical cavity pumped randomly with three two-level atom ensembles, and they explored the impact of various types of coherences of an arbitrary three-qubit state on the cavity field in the steady state. For thermalizing the cavity field and increasing its effective temperature with the coherences of three-qubit systems, they showed that—in contrast to quantum metrology—not the GHZ states but W states are useful [29]. Considering an ideal case with no decoherence on the atomic system, they also found that the optimal system of three qubits has a nearly equal mixture of a W state and a E state which consist of superpositions of one and two excitations, respectively, as will be detailed below.

Here, we consider a similar model where the cavity is pumped with fuel that consists of ensembles of four qubits instead of three qubits, as illustrated in Figure 1. We also consider realistic decoherence on the atomic system due to ambient temperature during the flight from the state preparation apparatus to the cavity. We design the state of the four-qubit fuel system, which includes a control parameter. By tuning the parameter according to the expected flight time, we show that the effect of decoherence on the quantum machine performance is almost eliminated.

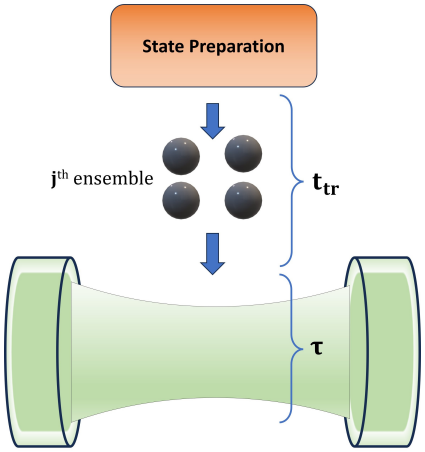

Figure 1. Four-atom ensembles are injected to the cavity in Poisson distribution. During the flight time, t_{tr}, atoms are subject to decoherence due to ambient temperature. Atoms interact with the cavity field during the transition time, τ. As shown in Figure 2, specific coherences of the atomic system might lead to pure thermalization of the cavity field, controlling its effective temperature.

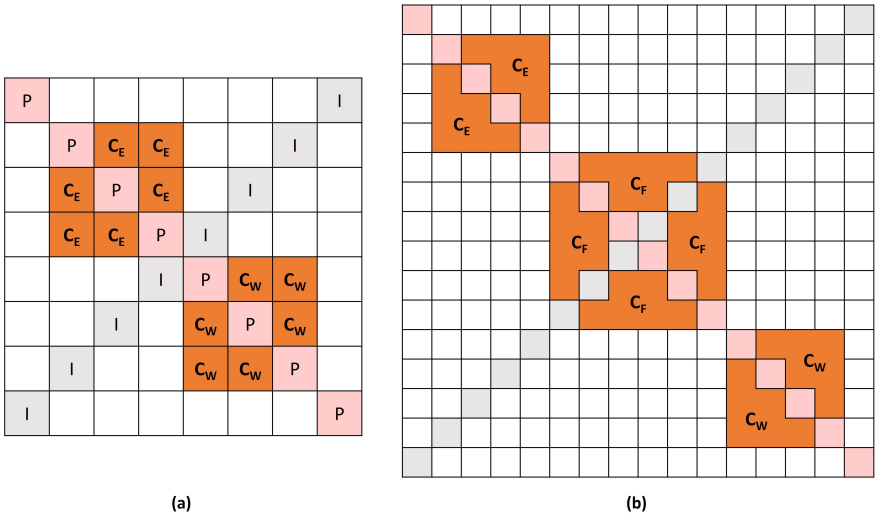

Figure 2. Heat exchange coherences of the density matrix of (**a**) three- and (**b**) four-qubit ensembles in the energy basis leading to pure thermalization of the cavity field.

This paper is organized as follows. In Section 2, we first present briefly the excitation basis we work in and the transformation between the excitation and the computational basis. We present the description of the quantum thermalization machine we consider and the role of the coherence terms of four-qubit states as well as the realistic assumptions and the conditions to satisfy for pure thermalization. In Section 3, we present the state of the four-qubits systems we construct as the optimal fuel, and we show how the machine performance can be protected from the devastating effects of natural decoherence. Finally, we present the Discussion in Section 4 and the Conclusions in Section 5.

2. Methods

2.1. Working Basis

Although the computational basis is usually preferred in quantum information studies, in this application area where excitations play a key role, it is more illuminating to work in the excitation basis or energy basis. Hence, we perform the following transformation from the computational basis to the energy basis, where $|e\rangle$ and $|g\rangle$ are encoded as $|0\rangle$, and $|1\rangle$, respectively. The following indices of the density matrix of the four-qubit system are changed as $4 \rightarrow 5;\ 5 \rightarrow 9;\ 6 \rightarrow 4;\ 7 \rightarrow 6;\ 8 \rightarrow 7;\ 9 \rightarrow 10,\ 10 \rightarrow 11,\ 11 \rightarrow 13,\ 12 \rightarrow 8,$ $13 \rightarrow 12$. As an example, the $m_{5,7}$ element in the computational basis corresponds to the $m_{9,6}$ element in the energy basis. The motivation and details of this transformation can be further found for systems up to three qubits in Ref. [29] and for four qubits in Ref. [61]. Note that alternative transformations can also be considered. Nevertheless, because not each term separately but rather the sum of terms in specific coherence groups are effective in controlling the cavity field, the result would not be different.

2.2. Quantum Thermalization Machine

The model we consider in this work is illustrated in Figure 1. Four-atom ensembles are prepared in a predetermined state and then injected to the cavity randomly, one ensemble at a time. Following Ref. [62], the distribution of the arrival time of the atomic ensembles to the cavity are designed to be Poissonian. The transfer time from the state preparation to the cavity is t_{tr}, and after interacting with the cavity field during τ, atomic ensembles exit the cavity.

The Tavis–Cummings model can describe the cavity–atomic ensemble interaction with the Hamiltonian H [63]. Let $\sigma_k^z, \sigma_k^+, and\ \sigma_k^-$ represent the z, raising and lowering Pauli operators for the kth atom, a and $a^\dagger$ represent the annihilation and creation operators for the cavity field, respectively, and g represent the coupling strength of atoms and photons

in the cavity. Denoting the Hamiltonians of the atomic ensemble, the cavity field and their interaction with $H_{\mathrm{a}}, H_{\mathrm{c}}$ and H_{int}, respectively, the Hamiltonian H can be written as

$$H = H_{\mathrm{a}} + H_{\mathrm{c}} + H_{\mathrm{int}}, \tag{1}$$

where

$$H_{\mathrm{a}} = \frac{\hbar\omega_a}{2}\sum_{k=1}^{4}\sigma_k^z, \tag{2}$$

$$H_{\mathrm{c}} = \hbar\omega_c a^\dagger a, \tag{3}$$

$$H_{\mathrm{int}} = \hbar g\sum_{k=1}^{4}(a\sigma_k^+ + a^\dagger\sigma_k^-). \tag{4}$$

We assume that the atomic transition frequency ω_a is resonant with the cavity frequency ω_c. In the interaction picture, the joint system of the atomic ensemble and the cavity evolve unitarily with $U(\tau) = \exp(-iH_{\mathrm{int}}\tau)$. Because we consider a repeated interaction of atomic ensembles with the cavity field, and we are interested in the cavity field after the transition of the jth atomic ensemble arriving at t_j and exiting at $t_j + \tau$, we trace out the atomic ensemble to obtain the cavity's state ρ_c as

$$\rho_c(t_j + \tau) = \mathrm{tr}_a[U(\tau)\rho_a \otimes \rho(t_j)U^\dagger(\tau)]. \tag{5}$$

One can also define a superoperator $\rho_c(t_j + \tau) \equiv S(\tau)\rho(t_j)$. Each atomic ensemble passes through the cavity in the interval $(t, t + \delta t)$ with probability $p\delta t$, and in the limit $\delta t \to 0$, the master equation of the cavity's state in terms of the jth atomic ensemble's state is found as [64,65]

$$\dot{\rho}_c = p\left[\sum_{i,j}^{16} a_{ij}\sum_{n=1}^{16} U_{ni}(\tau)\rho(t)[U_{nj}(\tau)]^\dagger - \rho(t)\right]. \tag{6}$$

Here, the elements of the density matrix of the atomic ensemble, ρ_a, are denoted as a_{ij}. In Refs. [29,61], the components under consideration are classified into distinct categories, namely populations (found in diagonal elements), ineffective terms (located in anti-diagonal elements), terms responsible for squeezing the cavity field, coherence displacement terms injecting coherence into the cavity, and heat exchange terms contributing to the pure thermalization of the cavity field. Our focus in this study is specifically on achieving the pure thermalization of the cavity field. To elaborate, apart from the elimination of squeezing terms, it is imperative that coherence displacement terms are also nullified, as the presence of coherence would disrupt the inherently chaotic nature of the cavity field, impeding the thermalization process.

Therefore, we restrict the density matrix of the four-qubit state to consist of heat exchange terms only plus the population terms required to construct a valid density matrix. Then, using the Lindbladian form [66], and assuming $g\tau \ll 1$, the master equation reduces to

$$\dot{\rho_c} \approx +\mathbb{L}_c\rho_c + \mathbb{L}\rho_c. \tag{7}$$

Here, the Lindbladian $\mathbb{L}_c$ describes the coupling of the cavity to the environment as [65]

$$\mathbb{L}_c\rho = \frac{1}{2}\kappa(\bar{n}_{\mathrm{th}} + 1)\mathbb{L}_d\rho + \frac{1}{2}\kappa\bar{n}_{\mathrm{th}}\mathbb{L}_e\rho, \tag{8}$$

where κ is the decay constant of the cavity, k_B is the Boltzmann constant, and $\bar{n}_{\mathrm{th}}$ is the average number of thermal photons in the environment at temperature T_{env},

$$\bar{n}_{\mathrm{th}} = \frac{1}{e^{\hbar\omega_c/k_BT_{\mathrm{env}}} - 1}. \tag{9}$$

With r_e and r_g representing the contributions of specific density matrix elements to the excitation and de-excitation, respectively, the Lindbladian $\mathbb{L}$ is given in terms of the incoherent excitation Lindbladian $\mathbb{L}_e = 2a^\dagger \rho a - aa^\dagger \rho - \rho aa^\dagger$, and de-excitation Lindbladian $\mathbb{L}_d = 2a\rho a^\dagger - a^\dagger a\rho - \rho a^\dagger a$, as

$$\mathbb{L}\rho = \mu\Big(\frac{r_e}{2}\mathbb{L}_e\rho + \frac{r_g}{2}\mathbb{L}_d\rho\Big). \tag{10}$$

2.3. Decoherence Channel

In quantum information, standard decoherence channels are usually considered such as dephasing, depolarizing, amplitude damping (ADC) and amplitude amplifying (AAC) [4]. In the present system, the generalized amplitude damping channel (GADC) [67] is considered to be applicable, which leads to both amplitude damping and amplitude amplifying due to ambient temperature [68]. With $\alpha = (\bar{n}_{\text{th}} + 1)/(2\bar{n}_{\text{th}} + 1)$ responsible for amplitude damping, and $\beta = \bar{n}_{\text{th}}/(2\bar{n}_{\text{th}} + 1)$ responsible for amplitude amplifying, the list of single-qubit Kraus operators acting on the qubits separately can be described in the computational basis as

$$\begin{aligned} K_{\text{GADC}} \quad = \quad & \{\sqrt{\alpha}\Big(|0\rangle\langle 0| + \sqrt{1-\bar{s}}|1\rangle\langle 1|\Big), \\ & \sqrt{\beta}\Big(\sqrt{1-\bar{s}}|0\rangle\langle 0| + |1\rangle\langle 1|\Big), \\ & \sqrt{\alpha p_{\text{GADC}}}|0\rangle\langle 1|, \\ & \sqrt{\beta p_{\text{GADC}}}|1\rangle\langle 0|\ \}. \end{aligned} \tag{11}$$

Here, the strength of the decoherence is $\bar{s} = 1 - \exp[-\gamma t_{\text{tr}}(1 + 2\bar{n}_{\text{th}})/2]$ where t_{tr} is the flight time as illustrated in Figure 1 and γ is the atomic damping rate [69].

2.4. Realistic Parameter Space

Parameters considering the realization of similar models have been explored in several works [29,30,61]. Hence, we take into account the same parameter space for our machine as $\kappa/\mu = 1$ with the resonance frequency $\omega_c/2\pi = 10$ GHZ and the ambient temperature $T_{\text{env}} \sim 160$ mK, which corresponds to $\bar{n}_{\text{th}} = 0.05$, and $\gamma/2\pi = 1$ MHZ would be a good choice [70]. Flight time t_{tr} is considered to be up to 50 ns, but we consider it up to 100 ns to have a clearer observation of the effect of decoherence.

3. Results

In the steady state below the master threshold, i.e., $r_e < r_g$, the solution of Equation (10) yields the effective temperature of the cavity T_{cav}

$$\frac{r_e + \bar{n}_{\text{th}}\kappa/\mu}{r_g + (\bar{n}_{\text{th}} + 1)\kappa/\mu} = e^{-\hbar\omega_c/k_B T_{cav}}, \tag{12}$$

and rearranging the term, one finds [61]

$$T_{cav} = \frac{\hbar\omega_c}{k_B}\left[\ln\left(\frac{R + \delta + 2C + 2(\bar{n}_{\text{th}} + 1)\kappa/\mu}{R - \delta + 2C + 2\bar{n}_{\text{th}}\kappa/\mu}\right)\right]^{-1}. \tag{13}$$

Here, $R = R_g + R_e = 4$ (which is equal to the number of qubits in the ensemble), $\delta = R_g - R_e$, $R_e = r_e - C$ and $R_g = r_g - C$, with

$$r_e = 4a_{11} + 3D_E + 2D_D + D_W + C \tag{14}$$

$$r_g = 4a_{16,16} + 3D_W + 2D_D + D_E + C \tag{15}$$

where

$$D_E = \sum_{i=2}^{5} a_{ii}, \quad D_D = \sum_{i=6}^{11} a_{ii}, \quad D_W = \sum_{i=12}^{15} a_{ii}, \tag{16}$$

$$C = C_E + C_F + C_W, \tag{17}$$

$$C_E = \sum_{i,j=2;\, i\neq j}^{5} a_{ij}, \tag{18}$$

$$C_F = \sum_{i,j=6;\, i\neq j}^{11} a_{ij} - \sum_{i,j=6}^{11} b_{ij}, \quad \text{and} \tag{19}$$

$$C_W = \sum_{i,j=12;\, i\neq j}^{15} a_{ij} \tag{20}$$

in the energy basis. Coherences C_E, C_F and C_W contribute to the heat exchange coherence C that leads to pure thermalization of the cavity field, controlling its effective temperature T_{cav}.

As illustrated in Figure 2, in the case of a 3-qubit system, the heat exchange coherence consists of only two blocks of density matrix elements, i.e., $C = C_E + C_W$, and the optimal state was found to be a nearly equal mixture of three-qubit E and W states, i.e., $\rho^3_{EW} = \frac{(1-\epsilon)|E^3\rangle\langle E^3| + (1+\epsilon)|W^3\rangle\langle W^3|}{2}$ with

$$|E^3\rangle = \frac{|001\rangle + |010\rangle + |100\rangle}{\sqrt{3}}, \quad |W^3\rangle = \frac{|110\rangle + |101\rangle + |011\rangle}{\sqrt{3}}. \tag{21}$$

in the computational basis. Here, a nonzero $0 < \epsilon \ll 1$ was considered because the decoherence of the atomic state during the flight to the cavity was ignored; therefore, the equal mixture of E and W with $\epsilon = 0$ does not satisfy the master threshold $r_e < r_g$. However, in the present work, because we consider a more realistic scenario including the atomic decoherence, $r_e < r_g$ is satisfied for $t_{tr} > 0$ for the state we engineer even in the case of equal mixture of the systems.

Expressing the states in the energy basis and providing illustrations of their corresponding density matrices, as depicted in Figure 2, is not only recommended for facilitating calculations but also enhances the clarity in visualizing the individual states' contributions to the desired coherence in heat exchange. The E and W components contribute to the C_E and C_W, respectively, in both three- and four-qubit systems. However, in the four-qubit case, there is also C_F (the central block).

So, we first ask what kind of four-qubit quantum system contributes to the C_F coherences without introducing any the squeezing or coherent-injection terms. And the crucial question is what kind of a potential mixture of that state with W and E systems would be optimal in the case of realistic decoherence.

To find an answer to the first question, because other states contain squeezing or coherence-injection terms, we consider four-qubit Dicke states with two excitations, as one and three excitation cases correspond to the $|E^4\rangle$ and $|W^4\rangle$ states, respectively. To find a state with elements in the central block of the density matrix in the energy basis corresponding to C_F terms, we consider the following parametric four-qubit state in the superposition of the two-excitation Dicke states

$$|F^4\rangle = a|0011\rangle + b|0101\rangle + c|0110\rangle + d|1001\rangle + e|1010\rangle + f|1100\rangle. \tag{22}$$

In the energy basis, the density matrix of the $|C^4\rangle$ state reads

$$|F^4\rangle\langle F^4| = \begin{pmatrix} 0&0&0&0&0&0&0&0&0&0&0&0&0&0&0&0\\ 0&0&0&0&0&0&0&0&0&0&0&0&0&0&0&0\\ 0&0&0&0&0&0&0&0&0&0&0&0&0&0&0&0\\ 0&0&0&0&0&0&0&0&0&0&0&0&0&0&0&0\\ 0&0&0&0&0&0&0&0&0&0&0&0&0&0&0&0\\ 0&0&0&0&0&a^2&ab&ac&ad&ae&af&0&0&0&0&0\\ 0&0&0&0&0&ab&b^2&bc&bd&be&bf&0&0&0&0&0\\ 0&0&0&0&0&ac&bc&c^2&cd&ce&cf&0&0&0&0&0\\ 0&0&0&0&0&ad&bd&cd&d^2&de&df&0&0&0&0&0\\ 0&0&0&0&0&ae&be&ce&de&e^2&ef&0&0&0&0&0\\ 0&0&0&0&0&af&bf&cf&df&ef&f^2&0&0&0&0&0\\ 0&0&0&0&0&0&0&0&0&0&0&0&0&0&0&0\\ 0&0&0&0&0&0&0&0&0&0&0&0&0&0&0&0\\ 0&0&0&0&0&0&0&0&0&0&0&0&0&0&0&0\\ 0&0&0&0&0&0&0&0&0&0&0&0&0&0&0&0\\ 0&0&0&0&0&0&0&0&0&0&0&0&0&0&0&0 \end{pmatrix}, \quad (23)$$

and the sum of heat exchange coherences reads $C = C_F = 2(ab + ac + bc + ad + bd + ae + ce + de + bf + cf + df + ef)$. Although not satisfying the master threshold as a pure state because $r_g = r_e$, we can check the contribution of each element to the cavity temperature by calculating T_{cav} in Equation (13)

$$T_{cav} = \frac{\hbar\omega_c}{k_B}\left[\ln\left(\frac{2 + C + 4\,\mathrm{Tr}(|F^4\rangle\langle F^4|)}{0.1 + C + 4\,\mathrm{Tr}(|F^4\rangle\langle F^4|)}\right)\right]^{-1}. \quad (24)$$

Having equal contribution to the heat exchange coherence and the cavity temperature, Equation (24) suggests equal parameters for the optimal state, i.e., $a = b = c = d = e = f = 1/\sqrt{6}$. If the atomic system in the pure $|F^4\rangle$ state satisfied the master threshold condition $r_g > r_e$, and if no decoherence on the system could be possible, the optimal state would be $|F^4\rangle$ so that the cavity temperature could reach $T_{cav} = 3.137$ K with $C = 4$. In other words, due to normalization of the density matrix to satisfy the unit trace, mixing F with E or W states degrades the performance of the quantum machine by decreasing the sum of heat exchange coherences and achieving a lower T_{cav}.

However, when F is subjected to the realistic decoherence due to ambient temperature during the flight, the value of the elements in the central block (with a through f) decreases, and new elements emerge in the upper left and lower right corners corresponding to mixing F with E and F states. Due to lengthy terms in the analytical solution after the application of Kraus operators in Equation (11), we consider an example with a 10 ns flight time, i.e., $t_{tr} = 10 \times 10^{-9}$ s. The pure $|F^4\rangle$ state evolves to a mixed state σ consisting of the element $\sigma_{16,16} = 0.00104758$ and the following three blocks as shown in Figure 2.

$$\sigma_E = \begin{bmatrix} 0.000721511 & 0.000480958 & 0.000480958 & 0.000480958\\ 0.000480958 & 0.000721511 & 0.000480958 & 0.000480958\\ 0.000480958 & 0.000480958 & 0.000721511 & 0.000480958\\ 0.000480958 & 0.000480958 & 0.000480958 & 0.000721511 \end{bmatrix}, \quad (25)$$

$$\sigma_F = \begin{bmatrix} 0.155587 & 0.155555 & 0.155555 & 0.155555 & 0.155555 & 0.155539\\ 0.155555 & 0.155587 & 0.155555 & 0.155555 & 0.155539 & 0.155555\\ 0.155555 & 0.155555 & 0.155587 & 0.155539 & 0.155555 & 0.155555\\ 0.155555 & 0.155555 & 0.155539 & 0.155587 & 0.155555 & 0.155555\\ 0.155555 & 0.155539 & 0.155555 & 0.155555 & 0.155587 & 0.155555\\ 0.155539 & 0.155555 & 0.155555 & 0.155555 & 0.155555 & 0.155587 \end{bmatrix}, \quad (26)$$

$$\sigma_W = \begin{bmatrix} 0.0156352 & 0.0104224 & 0.0104224 & 0.0104224 \\ 0.0104224 & 0.0156352 & 0.0104224 & 0.0104224 \\ 0.0104224 & 0.0104224 & 0.0156352 & 0.0104224 \\ 0.0104224 & 0.0104224 & 0.0104224 & 0.0156352 \end{bmatrix}, \tag{27}$$

As the contribution of σ_E block's coherences C_E to C is practically insignificant when compared to the contributions of C_F (due to the σ_F block) and C_W (due to the σ_W block), we focus on the F and W for engineering the optimal state under a realistic GADC.

Our aim is to eliminate the elements of the σ_W block which appear during the flight. Therefore, our strategy is to design a weighted classical mixture of F and W states such that the initially non-zero elements of the σ_W block approach zero due to the decoherence. With the E, F and W states under decoherence, the squeezing terms and the coherence-injection terms remain zero under GADC. However, the $r_g > r_e$ condition should be satisfied for the range of parameters.

For optimizing the performance of the machine, we propose the following parametric state for the four-qubit atomic system

$$\rho_\epsilon^0 = \epsilon\, |F^4\rangle\langle F^4| + (1-\epsilon)|W^4\rangle\langle W^4| \tag{28}$$

with the density matrix in the energy basis

$$\rho_\epsilon^0 = \begin{pmatrix}
0&0&0&0&0&0&0&0&0&0&0&0&0&0&0&0\\
0&0&0&0&0&0&0&0&0&0&0&0&0&0&0&0\\
0&0&0&0&0&0&0&0&0&0&0&0&0&0&0&0\\
0&0&0&0&0&0&0&0&0&0&0&0&0&0&0&0\\
0&0&0&0&0&0&0&0&0&0&0&0&0&0&0&0\\
0&0&0&0&0&\frac{\epsilon}{6}&\frac{\epsilon}{6}&\frac{\epsilon}{6}&\frac{\epsilon}{6}&\frac{\epsilon}{6}&\frac{\epsilon}{6}&0&0&0&0&0\\
0&0&0&0&0&\frac{\epsilon}{6}&\frac{\epsilon}{6}&\frac{\epsilon}{6}&\frac{\epsilon}{6}&\frac{\epsilon}{6}&\frac{\epsilon}{6}&0&0&0&0&0\\
0&0&0&0&0&\frac{\epsilon}{6}&\frac{\epsilon}{6}&\frac{\epsilon}{6}&\frac{\epsilon}{6}&\frac{\epsilon}{6}&\frac{\epsilon}{6}&0&0&0&0&0\\
0&0&0&0&0&\frac{\epsilon}{6}&\frac{\epsilon}{6}&\frac{\epsilon}{6}&\frac{\epsilon}{6}&\frac{\epsilon}{6}&\frac{\epsilon}{6}&0&0&0&0&0\\
0&0&0&0&0&\frac{\epsilon}{6}&\frac{\epsilon}{6}&\frac{\epsilon}{6}&\frac{\epsilon}{6}&\frac{\epsilon}{6}&\frac{\epsilon}{6}&0&0&0&0&0\\
0&0&0&0&0&\frac{\epsilon}{6}&\frac{\epsilon}{6}&\frac{\epsilon}{6}&\frac{\epsilon}{6}&\frac{\epsilon}{6}&\frac{\epsilon}{6}&0&0&0&0&0\\
0&0&0&0&0&0&0&0&0&0&0&\frac{1-\epsilon}{4}&\frac{1-\epsilon}{4}&\frac{1-\epsilon}{4}&\frac{1-\epsilon}{4}&0\\
0&0&0&0&0&0&0&0&0&0&0&\frac{1-\epsilon}{4}&\frac{1-\epsilon}{4}&\frac{1-\epsilon}{4}&\frac{1-\epsilon}{4}&0\\
0&0&0&0&0&0&0&0&0&0&0&\frac{1-\epsilon}{4}&\frac{1-\epsilon}{4}&\frac{1-\epsilon}{4}&\frac{1-\epsilon}{4}&0\\
0&0&0&0&0&0&0&0&0&0&0&\frac{1-\epsilon}{4}&\frac{1-\epsilon}{4}&\frac{1-\epsilon}{4}&\frac{1-\epsilon}{4}&0\\
0&0&0&0&0&0&0&0&0&0&0&0&0&0&0&0
\end{pmatrix}. \tag{29}$$

As the atomic ensemble exits the state preparation apparatus, due to interaction with the environment, the decoherence introduces the t_{tr} term in the density matrix which evolves as $\rho_\epsilon^0 \to \rho_{\epsilon,t_{tr}}$ during the flight to the cavity. Considering the realistic parameters presented in Section 2.4, we find

$$\begin{aligned} C &\approx \exp\left[-6.91\times 10^6\, t_{tr}\right](-2.385\times 10^{-18} - 3.532\times 10^{-17}\epsilon) \\ &+ \exp\left[-1.036\times 10^7 t_{tr}\right](-2.168\times 10^{-19} + 1.734\times 10^{-17}\epsilon) \\ &+ \exp\left[-3.455\times 10^6 t_{tr}\right](3+\epsilon), \end{aligned} \tag{30}$$

which reduces to $C \approx \exp\left[-3.455\times 10^6 t_{tr}\right](3+\epsilon)$ for reasonable flight times in the order of nanoseconds, and the cavity temperature

$$T_{cav} \approx 0.479\left[\ln\left(\frac{3245.1\exp\left[5.009\times 10^7 t_{tr}\right] + 7240.64\exp\left[5.355\times 10^7 t_{tr}\right]}{344.792\exp[5.355\times 10^7 t_{tr}] + \exp[5.009\times 10^7 t_{tr}](5678.93 + 2974.68\,\epsilon)}\right)\right]^{-1}, \tag{31}$$

and for the master threshold condition,

$$r_g - r_e \approx 3.63636 + \exp\left[-3.455 \times 10^6 t_{tr}\right](-1.63636 - 2\,\epsilon). \tag{32}$$

Let us first check the limit $t_{tr} \to 0$, yielding $C \to 3 + \epsilon$ which is valid for $r_g - r_e \to 2 - 2\epsilon$. Picking $\epsilon = 1 + \chi$ with $0 < \chi \ll 1$, $\rho_{\epsilon,t_{tr}}$ approaches the pure F state, bringing the effective temperature of the cavity $T_{cav} \to 3.137$ K.

For a finite t_{tr}, the optimal value of ϵ depends on t_{tr}. In Figure 3, we plot the cavity temperature in Equation (31) in the region satisfying the $r_g > r_e$ condition. We show that by tuning the control parameter ϵ of the initial state according to the expected flight time, the effect of the decoherence is almost reset, and the machine performance is almost not affected from the decoherence. In order to have a clearer perspective, we compare the machine performance between two scenarios where the atomic systems are prepared in the F state and in the ρ_ϵ^0 state. Although the F state is optimal in the $t_{tr} \to 0$ limit, it is vulnerable to the decoherence. As shown in Figure 4, in the case of realistic flight times, it degrades the machine performance significantly. In the second scenario preparing the atomic systems in the ρ_ϵ^0 state, we developed a numerical simulation for evaluating the machine performance. For every selected flight time t_{tr} with 10 ns intervals, we found the approximate maximum value of the parameter ϵ without violating the $r_g > r_e$ condition. This result clearly shows the advantage of engineering a state optimal for protecting the quantum thermalization machine performance against the decoherence on the atomic system due to realistic ambient temperature.

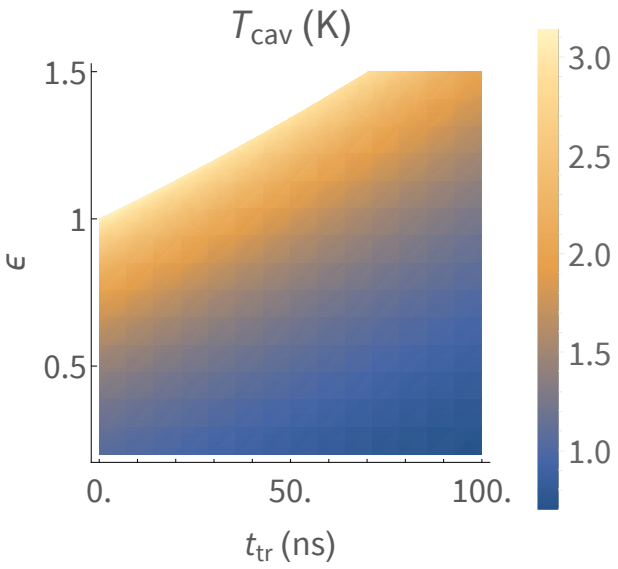

Figure 3. Effective temperature of the cavity T_{cav} in Kelvin as the KPI of the quantum thermalization machine performance due to repeated interactions with the injected four-qubit atomic ensembles. Atoms are subjected to generalized amplitude damping decoherence due to ambient temperature during their flight to the cavity. The strength of the decoherence increases with the flight time t_{tr}. However, tuning the control parameter ϵ of the state we design in Equation (28) according to the expected flight time, the effect of the decoherence on the quantum thermalization machine performance can almost be reset.

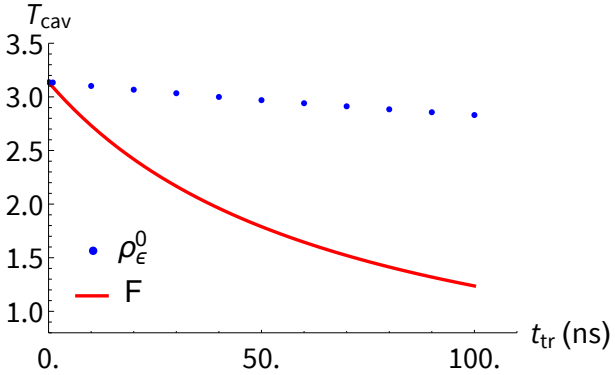

Figure 4. Quantum machine performance versus the flight time if the atomic system is prepared in the F or in the ρ_ϵ^0 state. While the decoherence on the F state significantly degrading the machine performance, tuning the control parameter ϵ protects the machine performance from the impact of the decoherence.

4. Discussion

Our method for finding a good quantum state for the four-qubit fuel to mitigate the impact of decoherence in this quantum task is not based on a search procedure, as it might be considered as the first choice. However, considering the computational complexity of searching for a goal state with a 16×16 density matrix in the Hilbert space satisfying several conditions for pure thermalization, we chose an alternative way. We performed a detailed observation of the impact of the decoherence on the density matrix and identified the evolution of the density matrix elements due to decoherence as a function of the flight time. With no decoherence in ideal conditions, the F state as the superposition of Dicke states as in Equation (23) would be the optimal state. However, we found that due to decoherence, elements in two blocks of the density matrix appear. These blocks correspond to density matrices of E and W states—the former being less significant on the machine performance. Hence, we designed a state ρ_ϵ^0 as a classical mixture of F and W, i.e., $\rho_\epsilon^0 = \epsilon\ |F^4\rangle\langle F^4| + (1-\epsilon)|W^4\rangle\langle W^4|$ where ϵ is utilized as the dynamical control parameter to fight the decoherence. Note that the E state could also be added to the mixture state for further improving the results, which we skipped for the sake of simplicity.

As a result of the proposed method for engineering the quantum state of the fuel of the quantum thermalization machine, the effective temperature of the cavity $T_{cav} = 3.137$ K for $t_{tr} = 0.1$ ns decreases only to $T_{cav} = 2.97$ K for the flight time $t_{tr} = 100$ ns, while it decreases to $T_{cav} = 1.2$ K without the engineering. In other words, although the effect of decoherence during the flight is not entirely eliminated, it is significantly reduced. However, we considered mixing the main state F with only the W state as in Equation (28) not only for simplicity but also because the contribution of the E state's terms due to decoherence is significantly less that the contribution of the W state's terms. Therefore, we do not exclude the possibility of reducing more or even eliminating the effect of the decoherence on the machine performance if the fuel state in Equation (28) is mixed also with the E state with a commensurate probability.

Observing quantum systems in Dicke states was discussed back in 1954 by R. Dicke [32]. Multipartite entangled W or E states as single-excitation instances of general Dicke states of any number of qubits can be prepared deterministically by following the methods in Refs. [40,71] and in particular for the two-level atoms as the qubits following the atom-cavity system designed in Refs. [72,73]. In Ref. [74], logic gates for generating arbitrary Dicke states of abstract qubits were studied. It would be interesting for future research to design an atom-cavity system as in Ref. [73] for generating the four-qubit atomic fuel system designed in the present work with the ability to tune the control parameter. While experimental realizations of these multipartite entanglement generation techniques become more difficult with increasing numbers of qubits, because the fuel system considered in this work requires only four qubits, it is within the reach of current technology.

Although the present work focused on engineering quantum systems of four qubits as the fuel for quantum thermalization machines or quantum heat engines, it can be easily adapted to any number of qubits by analyzing the heat-exchange coherence terms of the density matrix and the effect of the decoherence on the density matrix.

Our approach for designing the quantum resource for eliminating the effect of decoherence can also be considered in other applications in quantum thermodynamics as well as in a more general context in quantum information science.

For our mathematical model to be consistent with the physics of the quantum thermalization machine, the contribution of the specific terms of the fuel's density matrix leading to coherence injection to the cavity is required to be zero. Also, we ruled out the squeezing of the cavity field, so the contribution of the density matrix elements should be eliminated. Considering no coherence injection and no squeezing, in this work, we focused on the pure thermalization of the cavity field for increasing the effective temperature of the cavity T_{cav} beyond the environment's temperature, and T_{cav} is used as the KPI. However, quantum heat engines can be considered in the case of squeezing as well; therefore, a unique design of the quantum system could be interesting for future research.

5. Conclusions

We considered a four-qubit quantum system as the resource for fueling a quantum thermalization machine where the specific coherence terms can control the effective temperature of the machine. We considered realistic decoherence due to ambient temperature that significantly reduces the machine performance. For the four-qubit atomic fuel system, we designed a classical mixture of Dicke and W states where we utilize the mixture probability as the control parameter of the system to minimize the effect of the machine performance. Our work can be extended to quantum systems of an arbitrary number of qubits, and it can be considered in various other applications.

Author Contributions: Conceptualization, F.O. and R.S.; methodology, F.O. and R.S.; software, F.O. and V.B.; validation, F.O., R.S., V.B., C.B., A.A.A. and Ö.E.M.; formal analysis, F.O., R.S., V.B., C.B., A.A.A. and Ö.E.M.; investigation, F.O., R.S., V.B., C.B. and A.A.A.; resources, F.O., R.S., V.B., C.B. and A.A.A.; data curation, F.O. and V.B.; writing—original draft preparation, F.O., R.S., V.B., C.B., A.A.A. and Ö.E.M.; visualization, F.O., R.S. and V.B.; supervision, F.O., C.B., A.A.A. and Ö.E.M.; funding acquisition, F.O. and C.B. All authors have read and agreed to the published version of the manuscript.

Funding: This research was funded by the Personal Research Fund of Tokyo International University, Turkish Academy of Sciences (TÜBA)-Outstanding Young Scientist Award (GEBİP), and the Research Fund of the Istanbul Technical University with project codes: MGA-2022-43528, MDK-2021-42849.

Institutional Review Board Statement: Not applicable.

Informed Consent Statement: Not applicable.

Data Availability Statement: All the data in this study can be generated through the presented methods.

Conflicts of Interest: The authors declare no conflicts of interest.

References

1. Horodecki, R.; Horodecki, P.; Horodecki, M.; Horodecki, K. Quantum entanglement. *Rev. Mod. Phys.* **2009**, *81*, 865. [CrossRef]
2. Modi, K.; Brodutch, A.; Cable, H.; Paterek, T.; Vedral, V. The classical-quantum boundary for correlations: Discord and related measures. *Rev. Mod. Phys.* **2012**, *84*, 1655. [CrossRef]
3. Streltsov, A.; Adesso, G.; Plenio, M.B. Colloquium: Quantum coherence as a resource. *Rev. Mod. Phys.* **2017**, *89*, 041003. [CrossRef]
4. Nielsen, M.A.; Chuang, I.L. *Quantum Computation and Quantum Information: 10th Anniversary Edition*; Cambridge University Press: Cambridge, UK, 2011.
5. Madhok, V.; Datta, A. Quantum discord as a resource in quantum communication. *Int. J. Mod. Phys.* **2013**, *27*, 1345041. [CrossRef]
6. Dakić, B.; Lipp, Y.O.; Ma, X.; Ringbauer, M.; Kropatschek, S.; Barz, S.; Paterek, T.; Vedral, V.; Zeilinger, A.; Brukner, Č.; et al. Quantum discord as resource for remote state preparation. *Nat. Phys.* **2012**, *8*, 666–670. [CrossRef]

7. Deffner, S.; Campbell, S. *Quantum Thermodynamics: An introduction to the Thermodynamics of Quantum Information*; Morgan & Claypool Publishers: San Rafael, CA, USA, 2019. [CrossRef]
8. Kosloff, R. Quantum thermodynamics: A dynamical viewpoint. *Entropy* **2013**, *15*, 2100–2128. [CrossRef]
9. Horodecki, M. Reversible path to thermodynamics. *Nat. Phys.* **2008**, *4*, 833–834. [CrossRef]
10. Bender, C.M.; Brody, D.C.; Meister, B.K. Quantum mechanical Carnot engine. *J. Phys. Math. Gen.* **2000**, *33*, 4427. [CrossRef]
11. Abe, S. Maximum-power quantum-mechanical Carnot engine. *Phys. Rev.* **2011**, *83*, 041117. [CrossRef]
12. Scully, M.O.; Zubairy, M.S.; Agarwal, G.S.; Walther, H. Extracting Work from a Single Heat Bath via Vanishing Quantum Coherence. *Science* **2003**, *299*, 862–864. [CrossRef]
13. Quan, H.T.; Liu, Y.X.; Sun, C.P.; Nori, F. Quantum thermodynamic cycles and quantum heat engines. *Phys. Rev. E* **2007**, *76*, 031105. [CrossRef] [PubMed]
14. Thomas, G.; Das, D.; Ghosh, S. Quantum heat engine based on level degeneracy. *Phys. Rev. E* **2019**, *100*, 012123. [CrossRef] [PubMed]
15. Çakmak, S. Benchmarking quantum Stirling and Otto cycles for an interacting spin system. *JOSA B* **2022**, *39*, 1209–1215. [CrossRef]
16. Mukherjee, V.; Kofman, A.G.; Kurizki, G. Anti-Zeno quantum advantage in fast-driven heat machines. *Commun. Phys.* **2020**, *3*, 8. [CrossRef]
17. Bouton, Q.; Nettersheim, J.; Burgardt, S.; Adam, D.; Lutz, E.; Widera, A. A quantum heat engine driven by atomic collisions. *Nat. Commun.* **2021**, *12*, 2063. [CrossRef] [PubMed]
18. Horodecki, M.; Horodecki, P.; Horodecki, R. Mixed-state entanglement and distillation: Is there a "bound" entanglement in nature? *Phys. Rev. Lett.* **1998**, *80*, 5239. [CrossRef]
19. Werner, R.F.; Wolf, M.M. Bound entangled Gaussian states. *Phys. Rev. Lett.* **2001**, *86*, 3658. [CrossRef]
20. Yang, D.; Horodecki, M.; Horodecki, R.; Synak-Radtke, B. Irreversibility for all bound entangled states. *Phys. Rev. Lett.* **2005**, *95*, 190501. [CrossRef]
21. Horodecki, M.; Oppenheim, J.; Horodecki, R. Are the laws of entanglement theory thermodynamical? *Phys. Rev. Lett.* **2002**, *89*, 240403. [CrossRef]
22. Lavagno, A.; Scarfone, A.; Swamy, P.N. q-Deformed structures and generalized thermodynamics. *Rep. Math. Phys.* **2005**, *55*, 423–433. [CrossRef]
23. Lavagno, A.; Swamy, P.N. Generalized thermodynamics of q-deformed bosons and fermions. *Phys. Rev. E* **2002**, *65*, 036101. [CrossRef] [PubMed]
24. Ozaydin, F.; Müstecaplıoğlu, Ö.E.; Hakioğlu, T. Powering quantum Otto engines only with q-deformation of the working substance. *Phys. Rev. E* **2023**, *108*, 054103. [CrossRef] [PubMed]
25. Dillenschneider, R.; Lutz, E. Energetics of quantum correlations. *Europhys. Lett.* **2009**, *88*, 50003. [CrossRef]
26. Quan, H. Maximum efficiency of ideal heat engines based on a small system: Correction to the Carnot efficiency at the nanoscale. *Phys. Rev. E* **2014**, *89*, 062134. [CrossRef] [PubMed]
27. Lin, S.; Song, Z. Non-Hermitian heat engine with all-quantum-adiabatic-process cycle. *J. Phys. A Math. Theor.* **2016**, *49*, 475301. [CrossRef]
28. Gardas, B.; Deffner, S. Thermodynamic universality of quantum Carnot engines. *Phys. Rev. E* **2015**, *92*, 042126. [CrossRef] [PubMed]
29. Dağ, C.B.; Niedenzu, W.; Müstecaplıoğlu, Ö.E.; Kurizki, G. Multiatom quantum coherences in micromasers as fuel for thermal and nonthermal machines. *Entropy* **2016**, *18*, 244. [CrossRef]
30. Dag, C.B.; Niedenzu, W.; Ozaydin, F.; Müstecaplıoğlu, O.E.; Kurizki, G. Temperature control in dissipative cavities by entangled dimers. *J. Phys. Chem. C* **2019**, *123*, 4035–4043. [CrossRef]
31. Dür, W.; Vidal, G.; Cirac, J.I. Three qubits can be entangled in two inequivalent ways. *Phys. Rev. A* **2000**, *62*, 062314. [CrossRef]
32. Dicke, R.H. Coherence in spontaneous radiation processes. *Phys. Rev.* **1954**, *93*, 99. [CrossRef]
33. Raussendorf, R.; Briegel, H.J. A one-way quantum computer. *Phys. Rev. Lett.* **2001**, *86*, 5188. [CrossRef] [PubMed]
34. Brassard, G.; Broadbent, A.; Tapp, A. Quantum pseudo-telepathy. *Found. Phys.* **2005**, *35*, 1877–1907. [CrossRef]
35. Briegel, H.J.; Browne, D.E.; Dür, W.; Raussendorf, R.; Van den Nest, M. Measurement-based quantum computation. *Nat. Phys.* **2009**, *5*, 19–26. [CrossRef]
36. Zwerger, M.; Briegel, H.; Dür, W. Measurement-based quantum communication. *Appl. Phys. B* **2016**, *122*, 1–15. [CrossRef]
37. Tame, M.; Özdemir, Ş.; Koashi, M.; Imoto, N.; Kim, M. Compact Toffoli gate using weighted graph states. *Phys. Rev. A* **2009**, *79*, 020302. [CrossRef]
38. D'Hondt, E.; Panangaden, P. The computational power of the *W* and GHZ States. *Quantum Inf. Comput.* **2006**, *6*, 173–183. [CrossRef]
39. Ma, J.; Huang, Y.X.; Wang, X.; Sun, C. Quantum Fisher information of the Greenberger-Horne-Zeilinger state in decoherence channels. *Phys. Rev. A* **2011**, *84*, 022302. [CrossRef]
40. Ozaydin, F.; Yesilyurt, C.; Bugu, S.; Koashi, M. Deterministic preparation of W states via spin-photon interactions. *Phys. Rev. A* **2021**, *103*, 052421. [CrossRef]
41. Loss, D.; DiVincenzo, D.P. Quantum computation with quantum dots. *Phys. Rev. A* **1998**, *57*, 120. [CrossRef]
42. Häffner, H.; Roos, C.F.; Blatt, R. Quantum computing with trapped ions. *Phys. Rep.* **2008**, *469*, 155–203. [CrossRef]

43. Rotter, I.; Bird, J. A review of progress in the physics of open quantum systems: Theory and experiment. *Rep. Prog. Phys.* **2015**, *78*, 114001. [CrossRef]
44. Weimer, H.; Kshetrimayum, A.; Orús, R. Simulation methods for open quantum many-body systems. *Rev. Mod. Phys.* **2021**, *93*, 015008. [CrossRef]
45. Zhang, Q.; Xia, Y.J.; Man, Z.X. Effects of one-way correlations on thermodynamics of a multipartite open quantum system. *Phys. Rev. A* **2023**, *108*, 062211. [CrossRef]
46. Çakmak, S.; Türkpençe, D.; Altintas, F. Special coupled quantum Otto and Carnot cycles. *Eur. Phys. J. Plus* **2017**, *132*, 1–10. [CrossRef]
47. Türkpençe, D.; Müstecaplıoğlu, O.E. Quantum fuel with multilevel atomic coherence for ultrahigh specific work in a photonic Carnot engine. *Phys. Rev. E* **2016**, *93*, 012145. [CrossRef]
48. Gassab, L.; Pusuluk, O.; Müstecaplıoğlu, Ö.E. Geometrical optimization of spin clusters for the preservation of quantum coherence. *arXiv* **2023**, arXiv:2306.15232. [CrossRef]
49. Hardal, A.Ü.; Müstecaplıoğlu, Ö.E. Superradiant quantum heat engine. *Sci. Rep.* **2015**, *5*, 12953. [CrossRef]
50. Kim, J.; Oh, S.h.; Yang, D.; Kim, J.; Lee, M.; An, K. A photonic quantum engine driven by superradiance. *Nat. Photonics* **2022**, *16*, 707–711. [CrossRef]
51. Gallock-Yoshimura, K. Relativistic quantum Otto engine: Instant work extraction from a quantum field. *arXiv* **2023**, arXiv:2312.04485. https://doi.org/10.48550/arXiv.2312.04485.
52. Calderbank, A.R.; Shor, P.W. Good quantum error-correcting codes exist. *Phys. Rev. A* **1996**, *54*, 1098. [CrossRef]
53. Knill, E.; Laflamme, R. Theory of quantum error-correcting codes. *Phys. Rev. A* **1997**, *55*, 900. [CrossRef]
54. Lidar, D.A.; Chuang, I.L.; Whaley, K.B. Decoherence-free subspaces for quantum computation. *Phys. Rev. Lett.* **1998**, *81*, 2594. [CrossRef]
55. Yamamoto, T.; Hayashi, K.; Özdemir, Ş.K.; Koashi, M.; Imoto, N. Robust photonic entanglement distribution by state-independent encoding onto decoherence-free subspace. *Nat. Photonics* **2008**, *2*, 488–491. [CrossRef]
56. Bernu, J.; Deléglise, S.; Sayrin, C.; Kuhr, S.; Dotsenko, I.; Brune, M.; Raimond, J.M.; Haroche, S. Freezing coherent field growth in a cavity by the quantum Zeno effect. *Phys. Rev. Lett.* **2008**, *101*, 180402. [CrossRef] [PubMed]
57. Kondo, Y.; Matsuzaki, Y.; Matsushima, K.; Filgueiras, J.G. Using the quantum Zeno effect for suppression of decoherence. *New J. Phys.* **2016**, *18*, 013033. [CrossRef]
58. Yamamoto, T.; Shimamura, J.; Özdemir, Ş.; Koashi, M.; Imoto, N. Faithful qubit distribution assisted by one additional qubit against collective noise. *Phys. Rev. Lett.* **2005**, *95*, 040503. [CrossRef]
59. Mavadia, S.; Frey, V.; Sastrawan, J.; Dona, S.; Biercuk, M.J. Prediction and real-time compensation of qubit decoherence via machine learning. *Nat. Commun.* **2017**, *8*, 14106. [CrossRef]
60. Yu, W.; Chen, Y.; Zhang, C.; Chen, Y.; Wei, H.; Chen, Z.; Zhang, Y. A Software Architecting for Quantum Machine Learning Platform in Noisy Intermediate-Scale Quantum Era. *Res. Sq.* **2023**, *preprint*. [CrossRef]
61. Tuncer, A.; Izadyari, M.; Dağ, C.B.; Ozaydin, F.; Müstecaplıoğlu, O.E. Work and heat value of bound entanglement. *Quantum Inf. Process.* **2019**, *18*, 373. [CrossRef]
62. Meschede, D.; Walther, H.; Müller, G. One-atom maser. *Phys. Rev. Lett.* **1985**, *54*, 551. [CrossRef]
63. Tavis, M.; Cummings, F.W. Exact solution for an N-molecule—Radiation-field Hamiltonian. *Phys. Rev.* **1968**, *170*, 379. [CrossRef]
64. Filipowicz, P.; Javanainen, J.; Meystre, P. Theory of a microscopic maser. *Phys. Rev. A* **1986**, *34*, 3077. [CrossRef] [PubMed]
65. Liao, J.Q.; Dong, H.; Sun, C. Single-particle machine for quantum thermalization. *Phys. Rev. A* **2010**, *81*, 052121. [CrossRef]
66. Lindblad, G. On the generators of quantum dynamical semigroups. *Commun. Math. Phys.* **1976**, *48*, 119–130. [CrossRef]
67. Khatri, S.; Sharma, K.; Wilde, M.M. Information-theoretic aspects of the generalized amplitude-damping channel. *Phys. Rev. A* **2020**, *102*, 012401. [CrossRef]
68. Louisell, W.H. *Quantum Statistical Properties of Radiation*; John Wiley: Hoboken, NJ, USA, 1990.
69. Zhong, W.; Sun, Z.; Ma, J.; Wang, X.; Nori, F. Fisher information under decoherence in Bloch representation. *Phys. Rev. A* **2013**, *87*, 022337. [CrossRef]
70. Wallraff, A.; Schuster, D.I.; Blais, A.; Frunzio, L.; Majer, J.; Devoret, M.H.; Girvin, S.M.; Schoelkopf, R.J. Approaching unit visibility for control of a superconducting qubit with dispersive readout. *Phys. Rev. Lett.* **2005**, *95*, 060501. [CrossRef]
71. Yesilyurt, C.; Bugu, S.; Ozaydin, F.; Altintas, A.A.; Tame, M.; Yang, L.; Özdemir, S.K. Deterministic Local Doubling of W states. *J. Opt. Soc. Am. B* **2016**, *33*, 2313. [CrossRef]
72. Zang, X.P.; Yang, M.; Ozaydin, F.; Song, W.; Cao, Z.L. Generating Multi-Atom Entangled W States via Light-Matter Interface Based Fusion Mechanism. *Sci. Rep.* **2015**, *5*, 16245. [CrossRef]
73. Zang, X.P.; Yang, M.; Ozaydin, F.; Song, W.; Cao, Z.L. Deterministic Generation of Large Scale Atomic W States. *Opt. Exp.* **2015**, *24*, 12293. [CrossRef]
74. Kobayashi, T.; Ikuta, R.; Özdemir, Ş.K.; Tame, M.; Yamamoto, T.; Koashi, M.; Imoto, N. Universal gates for transforming multipartite entangled Dicke states. *New J. Phys.* **2014**, *16*, 023005. [CrossRef]

Disclaimer/Publisher's Note: The statements, opinions and data contained in all publications are solely those of the individual author(s) and contributor(s) and not of MDPI and/or the editor(s). MDPI and/or the editor(s) disclaim responsibility for any injury to people or property resulting from any ideas, methods, instructions or products referred to in the content.